Ocean Modelling 24 (2008) 65–71

Contents lists available at ScienceDirect

Ocean Modelling

journal homepage: www.elsevier.com/locate/ocemod

Short communication

Equatorial influence of QuikSCAT winds in an isopycnal ocean model compared to NCEP2 winds

ChuanLi Jiang [a,*], LuAnne Thompson [a], Kathryn A. Kelly [b]

[a] School of Oceanography, University of Washington, Box 357940, Seattle, WA 98195, United States
[b] Applied Physics Laboratory, University of Washington, Box 355640, Seattle, WA 98195, United States

ARTICLE INFO

Article history:
Received 16 April 2007
Received in revised form 29 April 2008
Accepted 8 May 2008
Available online 17 May 2008

ABSTRACT

An ocean model was used to examine whether the scatterometer winds can improve the model performance both dynamically and thermodynamically. Comparisons were done using QuikSCAT and NCEP2 winds for both the mean and variability from 2000 to 2004. The comparisons showed that the model forced by QuikSCAT winds gives more realistic mean SST, 20 °C isotherm depth (Z20), and latent heat flux than NCEP2 winds do. Sensitivity experiments indicated that QuikSCAT mean wind stress is important for the improved mean SST, Z20, and latent heat release to the atmosphere in the eastern Pacific. QuikSCAT wind speed, through its effect on the turbulent heat fluxes, is most important for the mean SST in the western Pacific. Finally, there were comparable correlations with observations of both SST and Z20 on the intra-seasonal time scale between the model forced with QuikSCAT winds and the model forced with NCEP2 winds.

1. Introduction

Accurate representation of ocean surface wind stress and wind speed is crucial for understanding the equatorial Pacific Ocean because surface winds govern both dynamical (through stress) and thermodynamical (through turbulent heat flux) processes. Numerical weather prediction (NWP) reanalysis winds, including NCEP reanalysis-2 (NCEP2, Kalnay et al., 1996; Kistler et al., 2001), are widely used in the modeling community because of their long and consistent time series and full spatial coverage. Since the SeaWinds scatterometer on QuikSCAT was launched in mid-July 1999, QuikSCAT winds have proved to be more accurate than NWP reanalysis winds when compared to TAO (tropical atmospheric-ocean) buoy winds (Kelly et al., 1999; Chelton et al., 2001; Jiang et al., 2005). They provide both high accuracy and high resolution dynamical forcing to drive ocean general circulation models (OGCM), but also give high quality hybrid turbulent heat fluxes in the tropical Pacific (Jiang et al., 2005; Ayina et al., 2006). For example, the time mean and standard deviation (STD) of 5 yr (January 2000–December 2004) QuikSCAT winds and NCEP2 winds are significantly different along the equatorial Pacific (Fig. 1). Mean zonal NCEP2 winds are generally weaker than QuikSCAT winds with differences in wind stress of up to 0.01 N m^{-2} in the central Pacific, and mean meridional wind stress east of 160°W is weaker by up to 0.005 N m^{-2}. QuikSCAT wind speed is measured relative to the moving ocean surface. The surface currents along the equator are about 1 m s^{-1} westward, with the winds in the same direction as the currents. Thus, we would expect that QuikSCAT would measure a smaller wind speed than NCEP2. However, mean NCEP2 wind speed is weaker than QuikSCAT by about 1 m s^{-1} almost all the way across the Pacific Ocean. In addition, the variability of NCEP2 is generally smaller than that of QuikSCAT winds, with the lack of variability of NCEP2 zonal wind stress and wind speed in the western Pacific (Fig. 1d and f) being particularly noteworthy. However, the variability of NCEP2 in the eastern Pacific is larger than that of QuikSCAT winds.

The impact of scatterometer winds in different OGCMs has been examined in some recent studies. Agarwal et al. (2006) compared the performance of a run forced by QuikSCAT winds with a run forced by NCEP/NCAR reanalysis winds in the modular ocean model from the geophysical fluid dynamics laboratory (GFDL). The surface currents (up to 150 m deep) simulated by QuikSCAT winds had less root-mean-square (RMS) error than those simulated by NCEP/NCAR winds. Meanwhile, the simulated Z20 in the QuikSCAT run agreed better with observations than in the NCEP/NCAR run. However, the mean SST in their QuikSCAT run had a cool bias, which was hypothesized to be owing to the physical inconsistencies between the wind field and turbulent heat fluxes. Several other studies have focused on the aspects of the wind stress relevant to ENSO (Wittenberg, 2004; Chen, 2003; Hackert et al., 2001). This paper is a precursor of an investigation of the roles of intra-seasonal Kelvin waves and tropical instability waves in SST variability along equatorial Pacific (Jiang et al., in preparation) that builds on previous work examining the factors controlling the heat budget along the equator in the tropical Pacific (Wang and McPhaden, 1999; McPhaden, 1993). The goal of this work is to examine the dynamical (by wind stress) and thermodynamical (by wind

* Corresponding author. Tel.: +1 206 685 7930.
E-mail address: chuanlij@ocean.washington.edu (C. Jiang).

1463-5003/$ - see front matter © 2008 Elsevier Ltd. All rights reserved.
doi:10.1016/j.ocemod.2008.05.003

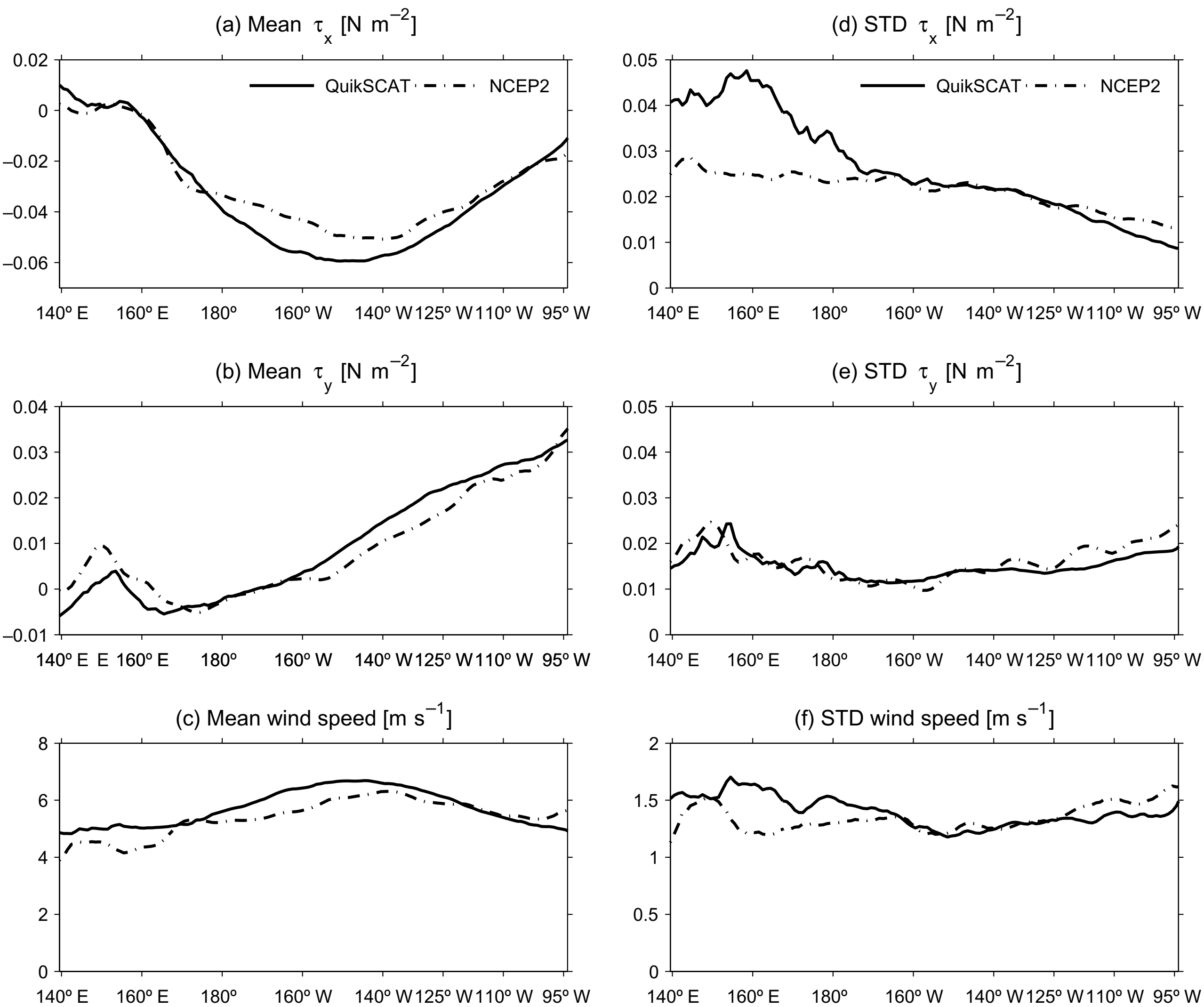

Fig. 1. Comparisons of 5-yr QuikSCAT (solid) with NCEP2 (dash-dot) winds along the equator (averaged from 2°S to 2°N) in the Pacific: mean (a) zonal wind stress, (b) meridional wind stress, (c) wind speed; standard deviation of (d) zonal wind stress, (e) meridional wind stress, and (f) wind speed.

speed) response of an OGCM in the equatorial Pacific to forcing by QuikSCAT and NCEP2 winds, and to determine if the differences in the two wind products cause quantifiably different performance in the ocean model.

2. Model description and data

The model we used is the GFDL Hallberg Isopycnal Model (HIM, Hallberg, 1997; Ladd and Thompson, 2002). This three-dimensional, isopycnal coordinate, C-grid general ocean circulation model implements a mixed-layer model based on that described in Oberhuber (1993), which is similar to the Kraus–Turner model except that the contribution to the entrainment velocity by wind mixing decays with mixed-layer depth. The model domain extended from 100°E to 70°W, 30°S to 30°N in the tropical Pacific, with grid spacing of 1° in longitude, 0.5° in latitude, and 16 layers in the vertical including an active mixed layer. The model was spun up for 10 years using ECMWF (European Centre for Medium-Range Weather Forecasts) 40 yr reanalysis (ERA40) forcing from January 1995 to December 1999 repeated once. Subsequently, two control runs were carried out for 5 yr from January 2000 to December 2004 using daily ISCCP (International Satellite Cloud Climatology Project) shortwave and longwave radiation, NCEP2 for other atmospheric state variables, and either (1) QuikSCAT wind stress and wind speed (run *Q*_Control of Table 1) or (2) NCEP2 wind stress and wind speed (run *N*_Control of Table 1).

QuikSCAT wind fields used in this study were produced by mapping the SeaWinds on QuikSCAT level 2B winds (http://podaac.jpl.nasa.gov) from swaths into daily fields on a $1^\circ \times 1^\circ$ grid, and using an objective averaging scheme with an approximate 4-day resolution (Kelly et al., 1999). Note that 4-day resolution global winds map is the best temporal resolution we can get from the QuikSCAT swaths to keep the error small and uniform following Schlax et al. (2001). The pseudostress is converted to stress from 10*m* vector wind components ($\vec{U_{10}}$) using $\vec{\tau} = \rho_a C_d \|\vec{U_{10}}\| \vec{U_{10}}$, with air density $\rho_a = 1.22$ kg/m^3 and wind speed $U = \|\vec{U_{10}}\|$ dependent drag coefficient $C_d = 0.001(2.7/U + 0.142 + 0.0764U)$ (Large et al., 1994). See Kelly et al. (1999) and Dickinson et al. (1998) for details on QuikSCAT wind speed and wind stress products. The evaluation of the QuikSCAT winds using TAO buoys in the equatorial Pacific showed that the QuikSCAT winds agreed well with TAO buoys (Kelly et al., 2001; Ebuchi et al., 2002; Jiang et al., 2005). NCEP2 daily winds and all other atmospheric variables were smoothed to 4-day temporal resolution using a similar weighting function to be consistent with the QuikSCAT winds. The turbulent heat fluxes, sensible (SHF) and latent heat flux (LHF), were calculated

Table 1
Sensitivity experiments and forcing used for wind stress and wind speed

Purpose	Name of experiment	Wind stress	Wind speed
Control run 1	Q_Control	QuikSCAT	QuikSCAT
Control run 2	N_Control	NCEP2	NCEP2
Wind stress vs wind speed	Q_{stress}_N_{speed}	QuikSCAT	NCEP2
	N_{stress}_Q_{speed}	NCEP2	QuikSCAT
Wind stress mean vs variability	$[\overline{Q}+N']_{stress}$_$Q_{speed}$	QuikSCAT mean + NCEP2 anom.	QuikSCAT
	$[\overline{N}+Q']_{stress}$_$Q_{speed}$	NCEP2 mean + QuikSCAT anom.	QuikSCAT

in the model using the University of Arizona bulk algorithm (Zeng et al., 1998) from either QuikSCAT or NCEP2 wind speed, NCEP2 atmospheric variables, and model SST. The sea surface salinity is restored to World Ocean Atlas (WOA) 2001 monthly climatology with a restoring time scale of 90 days. Sponge layers are used on the northern and southern boundaries to relax layer thickness, temperature and salinity to the WOA 2001 monthly climatology.

The model output was compared over the 5 yr period (January 2000– December 2004) with TAO array buoy measurements and TMI SST (tropical rainfall measuring mission microwave imager) data along the equator, averaged from 2°S to 2°N. It is noteworthy that microwave sensors measure ocean temperature slightly deeper (about 1–2 mm) than the skin temperature. Thus, there is a systematic bias between the mixed-layer model temperature (usually compared with TAO SST at 1 m) and TMI SST of about −0.1 °C, averaged over 64 buoys along the equatorial Pacific (Jiang et al., 2005). This paper focused more on the comparisons of SST bias owing to different wind products than on the absolute temperature bias between the model and TMI.

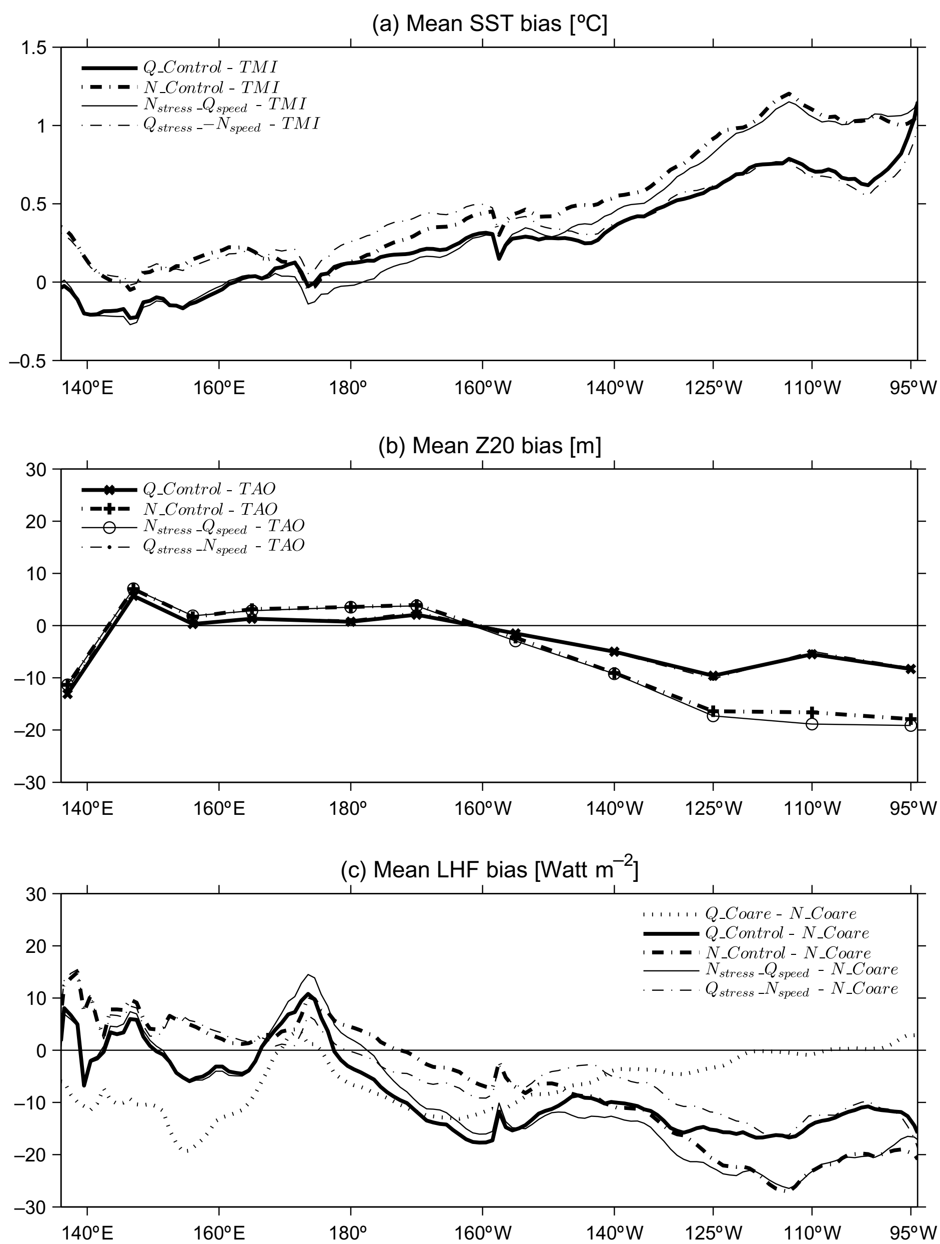

Fig. 2. Bias of 5-yr mean (a) SST relative to TMI, (b) Z20 relative to TAO, and (c) LHF relative to COARE product along the equator (averaged from 2°S to 2°N) from four model runs (see Table 1 for run descriptions). Negative bias in (b) indicates that the modeled Z20 is deeper than TAO. The negative bias in (c) indicates that the modeled LHF is stronger (more cooling) than *N*_Coare.

3. Results

Below we explore the differences in the two control runs forced by QuikSCAT (*Q*_Control) and NCEP2 winds (*N*_Control), respectively.

3.1. Time mean comparisons

The temporally averaged SST of the *Q*_Control run is closer to the averaged TMI SST than that of the *N*_Control run, especially in the central and eastern Pacific (Fig. 2a). The mean SST of the *Q*_Control run is slightly higher in the central and eastern Pacific and slightly lower in the far western Pacific than TMI, while the mean SST of the *N*_Control run is higher than TMI all along the equator. Note in particular the bias of more than 1 °C in the mean SST of the *N*_Control run around 110°W, compared with a bias of approximately 0.7 °C for *Q*_Control.

For the time mean Z20 (20 °C isotherm depth, always negative), the *Q*_Control run in general agrees well with that inferred from TAO sub-surface temperature, except in the eastern and far western Pacific where it is about 10*m* deeper than in the observations (Fig. 2b). The *N*_Control Z20 is slightly shallower than TAO in the west (except for 137°E) and 15–20 m deeper in the east. This gives a mean thermocline slope that is too small in the *N*_Control run compared to the observations and to the *Q*_Control run.

Turbulent heat fluxes (negative fluxes cool the ocean) in HIM were calculated from model SST, as is typical for OGCMs. As Seager et al. (1995) pointed out, this kind of bulk algorithm tends to constrain SST to observed values by specifying air temperature. Thus, a model run with higher SST than the observations would be expected to release more latent heat flux into the atmosphere than a run with realistic SST. The comparison of the mean SST must be combined with a comparison of the turbulent heat fluxes in the model runs to be able to evaluate model performance.

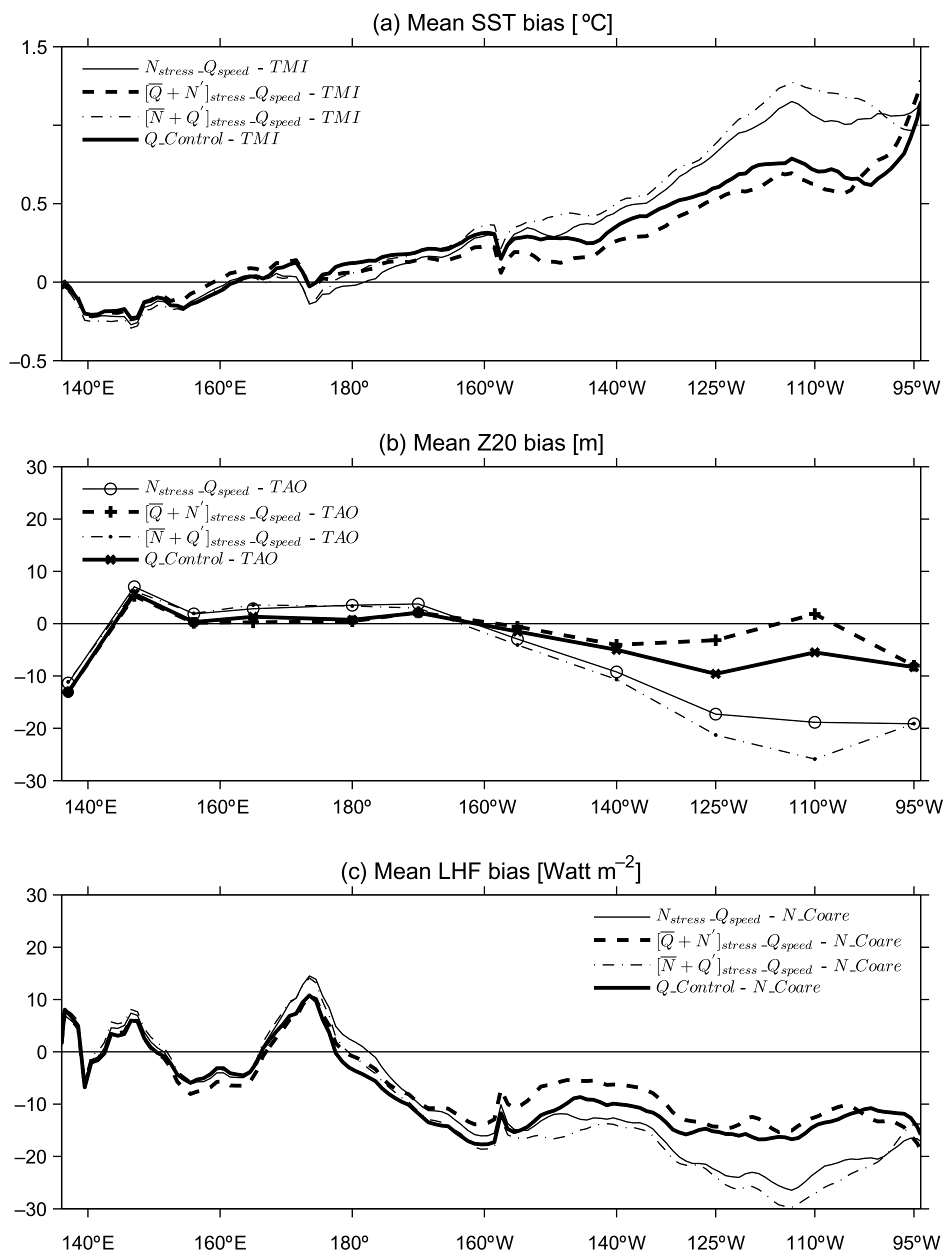

Fig. 3. Same as Fig. 2, but with different combinations of QuikSCAT and NCEP2 wind stress and their variability.

We compared latent heat flux from HIM (using model SST) with that calculated from TMI SST to determine how much the bulk algorithm of the model acts to modify the net heat flux into the ocean. This SST error that triggers the flux modification results from errors in the forcing fields as well as errors in model physics. Only LHF comparisons are examined here as SHF is much smaller in magnitude than LHF. Two LHF products were calculated using the COARE3.0a algorithm (Fairall et al., 2003), daily TMI SST, and other atmospheric variables from NCEP2: (1) with QuikSCAT wind speed (*Q*_Coare) and (2) with NCEP2 wind speed (*N*_Coare). As suggested by Jiang et al. (2005) and further analysis comparisons with the TAO buoys (2°S–2°N) from January 2000 to December 2001 (not shown), the RMS errors of *Q*_Coare and the *N*_Coare LHF estimates are comparable. However, the mean LHF of *N*_Coare is closer to that calculated using TAO measurements than *Q*_Coare, probably owing to the compensation in *N*_Coare between a low bias from low wind speed and a high bias from low air specific humidity (Jiang et al., 2005). Therefore, the mean LHF in *N*_Coare is used as the "true flux" for comparison to the LHF in the model runs discussed here.

The small wind speed differences between QuikSCAT and NCEP2 made little difference in the LHF between *Q*_Coare and *N*_Coare in the far eastern Pacific (east of 125°W), but the larger wind speed difference (about 1 m/s) west of 125°W led to a much larger LHF (about 10–20 W/m^{-2}) in *Q*_Coare relative to *N*_Coare (Fig. 2c). The LHF bias of the control run *N*_Control, relative to its corresponding COARE product *N*_Coare (Fig. 2c), is consistent with the positive SST bias of *N*_Control (Fig. 2a), where a positive SST bias in the eastern Pacific causes more heat flux out of the ocean. In the eastern Pacific, mean SST and LHF biases show the same relationship in both control runs, that is, the positive bias of SST causes the negative bias of LHF (more heat out of the ocean), with much larger magnitudes in the *N*_Control run than in *Q*_Control, that is, the bulk algorithm in the *N*_Control run had to compensate more for model errors owing to NCEP2 winds than for errors owing to QuikSCAT.

To examine the relative importance of QuikSCAT wind stress (through dynamical effects) and wind speed (through latent heat fluxes) in the improved performance of *Q*_Control over that in *N*_Control for mean SST, Z20 and LHF, we ran two additional experiments: Q_{stress}_N_{speed} and N_{stress}_Q_{speed} (Table 1), which combined QuikSCAT wind stress with NCEP2 wind speed, and NCEP2 wind stress with QuikSCAT wind speed, respectively. In the far eastern Pacific where NCEP2 and QuikSCAT mean wind speeds along the equator almost agree, *Q*_Control and Q_{stress}_N_{speed} (both using QuikSCAT wind stress) gave almost identical mean SST and LHF biases (Fig. 2a and c). *N*_Control and N_{stress}_Q_{speed} (both using NCEP2 wind stress) also gave similar results in the eastern Pacific, but showed larger biases than *Q*_Control and Q_{stress}_N_{speed}, except at 95°W. Even though the relative role of wind stress and wind speed for the mean SST and LHF in the far eastern Pacific cannot be determined (because the wind speeds are so similar in the two forcing products), the fact that QuikSCAT wind stress gives smaller biases than NCEP2 wind stress in mean SST and LHF indicates that QuikSCAT wind stress (through dynamical effects) is important for the improved model performance there. In the western Pacific, west of 170°E, the runs with the same wind speed (e.g., *N*_Control and Q_{stress}_N_{speed}) gave similar mean SST and LHF biases, which suggests the dominance of wind speed through its effect on the mean SST and latent heat fluxes there. The different roles of wind stress and wind speed at various locations along the equator are probably related to the slope of the mean thermocline depth, which is deep in the west and shallow in the east. Dynamics, that is, advection by surface currents, seems to be more important in the east (with a shallower thermocline) than in the west, consistent with the work of Wang and McPhaden (1999).

The two runs using QuikSCAT wind stress (*Q*_Control and Q_{stress}_N_{speed}) gave almost identical mean Z20 along the equator, and the two runs using NCEP2 wind stress (*N*_Control and N_{stress}_Q_{speed}) gave similar results, but with a much larger bias (deeper) east of 160°W. The runs using NCEP2 wind stress have a much smaller mean thermocline slope than the two runs using QuickSCAT wind stress, which suggests that QuikSCAT wind stress is responsible for the better representation of Z20, especially east of 160°W.

Given the success of QuikSCAT wind stress in modeling the mean SST, Z20 and LHF in the eastern Pacific, we further examined the relative importance of the mean and variability of QuikSCAT wind stress. We ran another two experiments: $[\overline{Q}+N']_{stress}$_$Q_{speed}$ and $[\overline{N}+Q']_{stress}$_$Q_{speed}$ (Table 1), in which we substitute the

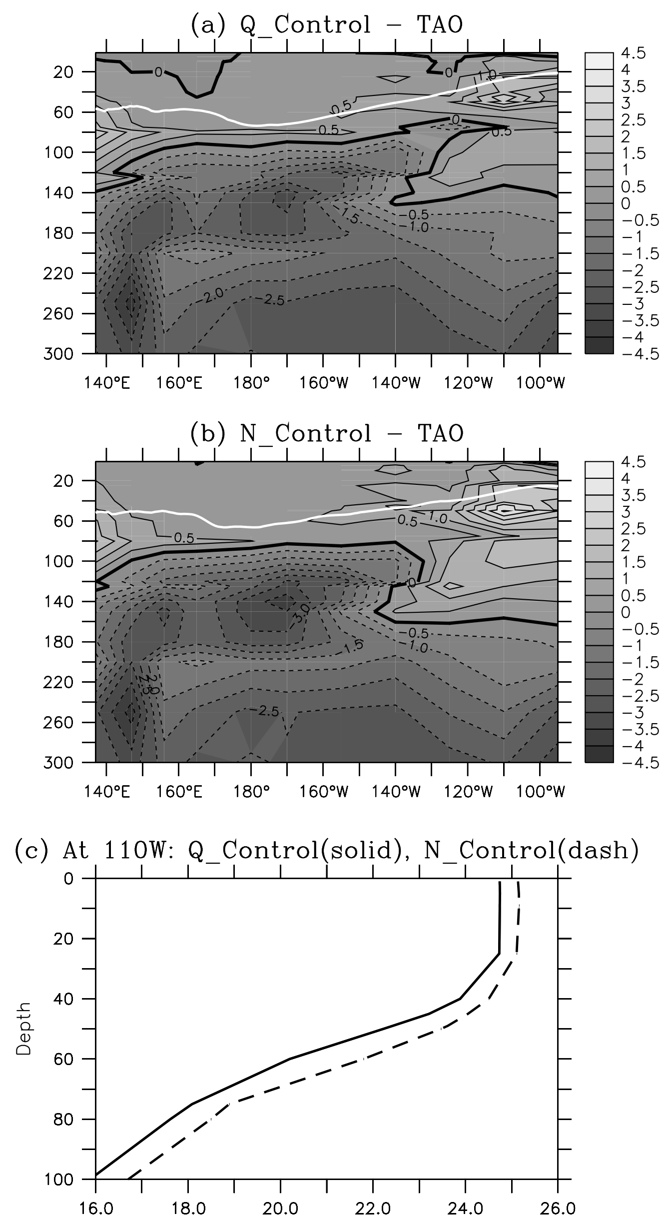

Fig. 4. (a) Bias of 5-yr mean sub-surface temperature of *Q*_Control run relative to TAO, (b) bias of 5-yr mean sub-surface temperature of *N*_Control run relative to TAO, and (c) five-year mean sub-surface temperature profiles at 110°W for the *Q*_Control run (solid) and the *N*_Control run (dash). The white solid lines in (a) and (b) are the mean mixed-layer depths for *Q*_Control and *N*_Control run, respectively. Units are °C.

variability of the wind stress in one product with the variability of the other product. In the central and eastern Pacific, Q_Control and $[\overline{Q}+N']_{\text{stress}}$_$Q_{\text{speed}}$ (thick dashed lines in Fig. 3), which have the same QuikSCAT mean wind stress, gave similar mean SST, Z20, and LHF biases. At the same time, N_{stress}_Q_{speed} and $[\overline{N}+Q']_{\text{stress}}$_$Q_{\text{speed}}$ (Fig. 3), both with mean NCEP2 wind stress, gave similar results, but with much larger biases than Q_Control and $[\overline{Q}+N']_{\text{stress}}$_$Q_{\text{speed}}$. This indicates that QuikSCAT mean wind stress is more crucial in producing realistic mean SST, Z20, and LHF in the central and eastern Pacific than either the seasonal cycle or higher frequency variability.

Vertical entrainment (a net cooling term) and net heating (a net warming term) dominate the mean mixed-layer temperature budget in the eastern Pacific (not shown). The Q_Control run has both a larger vertical temperature gradient of the temperature at the base of the mixed layer (Fig. 4c) and larger entrainment velocity than in the N_Control run, indicating that the entrainment would cool the ocean more in the Q_Control run. Meanwhile, the Q_Control run also has a shallower mixed-layer depth (Fig. 4a and b) and less latent heat loss (Fig. 2c) than in the N_Control run, indicating that the heating would warm the ocean more in the Q_Control run. However, the differences between the two runs are dominated by the differences in the entrainment, instead of by the heating, giving a lower mean SST in the Q_Control run in the eastern Pacific (Fig. 2a).

3.2. Intra-seasonal comparisons

To compare the intra-seasonal (33–88 days) (Jiang et al., in preparation) response of the two control runs (QuikSCAT and NCEP2) to winds, we calculated the correlations of intra-seasonal Z20 and SST with TAO measurements along the equator for Q_Control *and* N_Control runs. Correlations with the observations for the Q_Control were comparable to those for the N_Control run (Fig. 5).

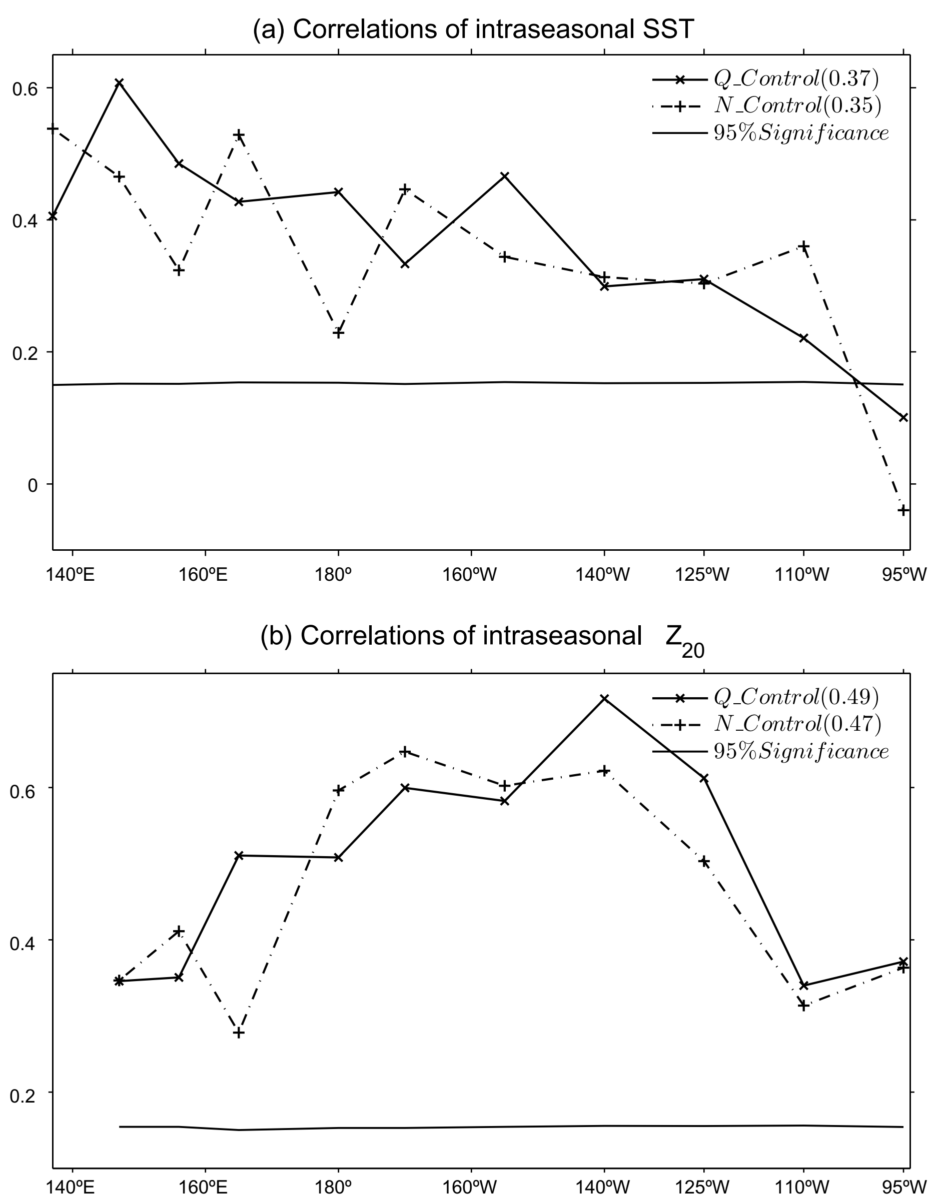

Fig. 5. Correlations of the intra-seasonal signals with TAO observations over 10 TAO locations along the equator (averaged from 2°S to 2°N) between Q_Control run and N_Control run for (a) SST and (b) Z20. Experiments designations are listed in legends and are described in Table 1.

Averaged over 11 TAO locations, the correlations were 0.37 for SST and 0.49 for Z20 for the *Q*_Control, compared with 0.35 for SST and 0.47 for Z20 for the *N*_Control run.

4. Summary and discussion

Using an isopycnal ocean model along the equatorial Pacific, we examined the sensitivity of the mean and variability of the upper ocean to two different wind stress and wind speed products; in particular, we wished to determine whether the QuikSCAT winds can improve the model performance both dynamically and thermodynamically.

The model run with QuikSCAT winds had more realistic mean SST, Z20, sub-surface temperature and latent heat flux loss than the run with NCEP2 winds, especially in the central and eastern pacific. The mean SST and sub-surface temperature in the *N*_Control run have larger warm biases, which trigger the bulk algorithm to release more latent heat out of the ocean. Meanwhile, the mean thermocline slope is much smaller in the *N*_Control run when compared to both the observations and the *Q*_Control run. Sensitivity experiments revealed that the mean QuikSCAT wind stress is important in reproducing observed mean SST, Z20 and sub-surface temperature in the eastern Pacific, and results in more realistic latent heat flux into the atmosphere.

The run with QuikSCAT winds had slightly larger correlations with observations of intra-seasonal Z20 and SST along the equator than the run with NCEP2 winds, which suggests that QuikSCAT winds and NCEP2 winds will produce a comparably realistic intra-seasonal mixed-layer temperature budget anomaly terms.

Since our study only focused on the equatorial Pacific in a single ocean model, its conclusions can not be generalized to the off-equatorial Pacific regions and to other numerical models. However, in a recent study, Agarwal et al. (2006) compared the performance of QuikSCAT winds with NCEP/NCAR winds in a different OGCM. The surface currents and Z20 in the QuikSCAT run have better agreement with observations than the NCEP/NCAR run, which is consistent with the results of this study. The better performance of NCEP/NCAR forcing in reproducing SST in the eastern Pacific might be in part owing to the weak NCEP/NCAR shortwave heat flux compensating for the weak NCEP/NCAR winds to give a smaller SST bias.

Acknowledgements

The authors thank Suzanne Dickinson for preparing the QuikSCAT gridded winds and NCEP2 fields, and David Darr for the help in model. This work was supported by NASA's Ocean Vector Winds Science Team through Contract 1285662 with the Jet Propulsion Laboratory.

References

Agarwal, N., Sharma, R., Basu, S.K., Sarkar, A., Agarwal, V.K., 2006. Evaluation of relative performance of QuikSCAT and NCEP re-analysis winds through simulations by an OGCM. Deep Sea Res. Part I 54 (8), 1311–1328.
Ayina, L.-H., Bentamy, A., Mestas-Nunez, A.M., Madec, G., 2006. The impact of satellite winds and latent heat fluxes in a numerical simulation of the tropical Pacific Ocean. J. Climate 19, 5889–5902.
Chelton, D.B., Esbensen, S.K., Schlax, M.G., Thum, N., Freilich, M.H., 2001. Observations of coupling between surface wind stress and sea surface temperature in the eastern tropical Pacific. J. Climate 14, 1479–1498.
Chen, D., 2003. A comparison of wind products in the context of ENSO prediction. Geophys. Res. Lett. 30 (3), 1107. doi:10.1029/2002GL016121.
Dickinson, S., Singh, S., Kelly, K.A., Spillane, M., McPhaden, M.J., 1998. Establishing a mapping methodology for NSCAT winds. Technical Report APL-UW TR 9801, Appl. Phys. Lab., University of Washington, Seattle.
Ebuchi, N., Graber, H.C., Caruso, M.J., 2002. Evaluation of wind vectors observed by QuikSCAT/SeaWinds using ocean buoy data. J. Atmos. Ocean. Technol. 19, 2049–2062.
Fairall, C.W., Bradley, E.F., Hare, J.E., Grachev, A.A., Edson, J.B., 2003. Bulk parameterization of air-sea fluxes: updates and verification for the COARE algorithm. J. Climate 16, 571–591.
Hackert, E.C., Busalacchi, A.J., Murtugudde, R., 2001. A wind comparison study using an ocean general circulation model for the 1997–1998 El Nio. J. Geophys. Res. 106, 2345–2362.
Hallberg, R., 1997. Localized coupling between surface and bottom intensified flow over topography. J. Phys. Oceanogr. 27 (27), 911–988.
Jiang, C., Cronin, M.F., Kelly, K.A., Thompson, L., 2005. Evaluation of a hybrid satellite- and NWP-based turbulent heat flux product using tropical atmosphere-ocean (TAO) buoys. J. Geophys. Res. 110, C09007. doi:10.1029/2004JC002824.
Jiang, C., Thompson, L., Kelly, K.A., Cronin, M.F. The roles of intra-seasonal Kelvin waves and tropical instability waves in SST variability along equatorial Pacific in an isopycnal ocean model, in preparation.
Kalnay, E. et al., 1996. The NCEP/NCAR 40-year reanalysis project. Bull. Am. Meteorol. Soc. 77, 437–471.
Kelly, K.A., Dickinson, S., Yu, Z.-J., 1999. NSCAT tropical wind stress maps: implications for improving ocean modeling. J. Geophys. Res. 104, 11291–11310.
Kelly, K.A., Dickinson, S., McPhaden, M.J., Johnson, G., 2001. Currents evident in Satellite wind data. Geophys. Res. Lett. 28 (12), 2469–2472.
Kistler, R. et al., 2001. The NCEP-NCAR 50-year reanalysis: monthly means CD-ROM and documentation. Bull. Am. Meteorol. Soc. 82, 247–268.
Ladd, C., Thompson, L., 2002. Decadal variability of North Pacific central mode water. J. Phys. Oceanogr. 32, 2870–2881.
Large, W.G., McWilliams, J.C., Doney, S.C., 1994. Oceanic vertical mixing: a review and a model with a vertical *K*-profile boundary layer parameterization. Rev. Geophys., 363–403.
McPhaden, M.J., 1993. Mixed layer temperature balance on intraseasonal timescales in the equatorial Pacific Ocean. J. Climate 15, 2632–2647.
Oberhuber, J., 1993. Simulation of the Atlantic circulation with a coupled sea ice-mixed layer-isopycnal general circulation model. Part I: model description. J. Phys. Oceanogr. 23, 808–829.
Schlax, M.D., Chelton, D.B., Freilich, M.H., 2001. Sampling errors in wind fields constructed from single and tandem scatterometer data sets. J. Atmos. Ocean. Technol. 10, 1014–1036.
Seager, R., Kushnir, Y., Cane, M.A., 1995. On heat flux boundary conditions for ocean models. J. Phys. Oceanogr. 25, 3219–3230.
Wang, W., McPhaden, M.J., 1999. The surface-layer heat balance in the equatorial Pacific Ocean. Part I: mean seasonal cycle. J. Phys. Oceanogr. 29, 1812–1831.
Wittenberg, A.T., 2004. Extended wind stress analyses for ENSO. J. Climate 17, 2526–2540.
Zeng, X., Zhao, M., Dickinson, R.E., 1998. Intercomparison of bulk aerodynamic algorithms for the computation of sea surface fluxes using TOGA COARE and TAO data. J. Climate 11, 2628–2644.